IEEE Access
Multidisciplinary | Rapid Review | Open Access Journal

Received June 8, 2020, accepted July 17, 2020, date of publication July 21, 2020, date of current version July 31, 2020.

Digital Object Identifier 10.1109/ACCESS.2020.3010847

ScalpEye: A Deep Learning-Based Scalp Hair Inspection and Diagnosis System for Scalp Health

WAN-JUNG CHANG[1,2], (Member, IEEE), LIANG-BI CHEN[1,2], (Senior Member, IEEE), MING-CHE CHEN[1,2], (Member, IEEE), YI-CHAN CHIU[1,3], AND JIAN-YU LIN[1]

[1]Department of Electronic Engineering, Southern Taiwan University of Science and Technology, Tainan 71005, Taiwan
[2]AIoT Innovation Technology and Experience Design Center (AIoT Center), Southern Taiwan University of Science and Technology, Tainan 71005, Taiwan
[3]Electrical Engineering and Electronics Program, Graduate School of Engineering, Kogakuin University of Technology and Engineering, Tokyo 163-8677, Japan

Corresponding author: Wan-Jung Chang (allenchang@stust.edu.tw)

This work was supported in part by the Ministry of Science and Technology (MoST), Taiwan, under Grant MOST 107-2637-E-218-003, Grant MOST 108-2637-E-218-004, Grant MOST 108-2622-8-218-004-TE2, and Grant MOST 109-2622-8-218-004-TE2, in part by the Ministry of Education (MoE) through the Advanced Intelligent Biomedical Allied Research Center, Higher Education Sprout Project, Taiwan, under Grant 1300-107P735, in part by the HairING Health Chain Group, Taiwan, and in part by the Milan Fashion Hair Group, Tainan, Taiwan.

ABSTRACT Many people suffer from scalp hair problems such as dandruff, folliculitis, hair loss, and oily hair due to poor daily habits, imbalanced nutritional intake, high stress, and toxic substances in their environment. To treat these scalp problems, dedicated services such as scalp hair physiotherapy have emerged in recent years. This article proposes a deep learning-based intelligent scalp inspection and diagnosis system, named ScalpEye, as an efficient inspection and diagnosis system for scalp hair physiotherapy as part of scalp healthcare. The proposed ScalpEye system consists of a portable scalp hair imaging microscope, a mobile device app, a cloud-based artificial intelligence (AI) training server, and a cloud-based management platform. The ScalpEye system can detect and diagnose four common scalp hair symptoms (dandruff, folliculitis, hair loss, and oily hair). In this study, we tested several popular object detection models and adopted a Faster R-CNN with the Inception ResNet_v2_Atrous model in the ScalpEye system for image recognition when inspecting and diagnosing scalp hair symptoms. The experimental results show that the ScalpEye system can diagnose four common scalp hair symptoms with an average precision (AP) ranging from 97.41% to 99.09%.

INDEX TERMS Artificial intelligence over the Internet of Things (AIoT), deep learning, image processing, image recognition, inspection, haircare, healthcare, scalp hair diagnosis.

I. INTRODUCTION

Many people suffer from scalp hair related problems such as dandruff, folliculitis, hair loss, and oily hair for reasons that include poor daily habits, imbalanced nutritional intake, high stress, and toxic substances in their environments. At least 30% of these problems result in hair loss. Rajput [1] evaluated the causes and clinical expressions of hair loss due to air pollution.

The World Health Organization (WHO) reported [2] that approximately 70% of adults have scalp hair problems. The causes of scalp hair problems include endocrine, genetic, disease, or other internal factors. Misery *et al.* [3] evaluated the severity of sensitive scalps and symptomatology by adopting a severity score of abnormal sensations. Misery *et al.* [4] found that dandruff, scalp pruritus, and related symptoms occur in the French population. Other related studies in children conducted in the USA and Australia have shown that dandruff is present in 18% of children. Therefore, both adults and children can have scalp hair problems [5].

Hence, how to effectively prevent scalp hair-related problems and scalp hair maintenance are important. To process such increasingly serious scalp problems, dedicated services, including scalp hair physiotherapy, have emerged in recent years.

Under the current most common processing procedures in scalp hair physical therapy, the condition of the patient's scalp hair is determined by manual inspection. However, such

The associate editor coordinating the review of this manuscript and approving it for publication was Shangce Gao.

manual inspections are dependent on the skill level of the physiotherapist; thus, they can lead to different results and concerns regarding the scalp hair condition and the diagnosis.

Consequently, two key problems exist related to haircare services in the current hairdressing industry, which are summarized below.

1) THE EXTREMELY HIGH COST OF EDUCATION AND TRAINING

In contrast to ordinary hairdressers, scalp hair physiotherapists must be able to determine the scalp hair health condition of the customer's scalp hair directly from microscopy images. These images are acquired by a dedicated inspection instrument and can reveal the current status of internal and external factors affecting scalp hair health. Acquiring such skill takes at least a half-year of education and training. Generally, the training cost is 14,000 U.S. dollars for each new employee in the hairdressing industry in Taiwan. However, the frequent turnover of employees in the hairdressing industry has led to companies investing considerable time and cost due to the need to continuously cultivate physiotherapist skillsets.

2) THE INTERPRETATION OF SCALP HEALTH CONDITION VARIES BETWEEN INDIVIDUALS

The interpretation of scalp hair microscopy images differs among professional physiotherapists even when they have received the same professional training. Such differences in diagnostic result interpretation also occur due to lack of experience. Confusion often occurs between customers and hairdressing companies, highlighting the need for a scientific and systematic quantitative benchmark.

To overcome the two abovementioned problems, we propose a deep learning-based intelligent scalp inspection and diagnosis system, named ScalpEye, to inspect and diagnose four common scalp hair symptoms in scalp healthcare: dandruff, folliculitis, hair loss, and oily hair.

The proposed ScalpEye system main provides the following main contributions:

- It reduces the high cost and time of education and training for scalp hair physiotherapists.
- It reduces the mistakes and inconsistent judgments of different human interpreters.
- It provides an automatic and highly accurate AI-based recognition method whereby people can know their current status of scalp hair health problems.
- The diagnosis result from each scalp hair inspection can be sent to an online cloud-based management platform, which can help related enterprises (such as scalp hair therapy and beauty salons) track the progress of scalp hair care, treatments, and customer therapies.
- It maintains cloud-based scalp hair records for customers, helping scalp hair physiotherapist regularly track and analyze the scalp hair health status their customers.
- The proposed cloud-based management platform efficiently manages customer memberships.

The remainder of this article is organized as follows. Related works are reviewed in Section II. The proposed ScalpEye system is described in Section III. Section IV describes a prototype of the proposed ScalpEye system and reports the experimental results. Finally, we conclude the study in Section V.

II. RELATED WORKS

Some recent previous works [8]–[26] have been reported that focus on detecting the status of skin or scalp hair. To the best of our knowledge, most of these previous works have focused on skin inspection or on diagnosing various conditions, such as skin lesions, skin cancer, monitoring skin recovery, and noninvasive diagnosis of skin burn injuries. However, studies related to scalp hair issues are sparse to date. The related literature [16]–[26] on scalp hair issues is reviewed and introduced as follows.

Lacarrubba *et al.* [16] demonstrated that scalp hair dermoscopy (also known as scalp image microscopy) is a useful tool for monitoring symptoms of scalp hair and skin and treating conditions. Rudnicka *et al.* [17] used trichoscopy, which involves dermoscopy of both hair and scalp to diagnose hair and scalp diseases such as tinea capitis, alopecia areata, and trichotillomania. Kim *et al.* [18] evaluated hair and scalp conditions based on microscopy image measurements and analysis.

Shih [19], Shih and Lin [20] developed an automatic hair segmentation and counting system based on unsupervised learning that reduced the time required to assess scalp hair compared with that required for a human inspection. Three processing flows were designed to overcome three problems: double-counting of some hairs, nonstraight hair detection, and accurately locating all hairs. Benhabiles *et al.* [21] adopted a deep learning-based matching method to predict the level of hair loss. The matching method classifies hair loss images using the Hamilton–Norwood scaling model.

Lee and Yang [22] proposed an intelligent hair and scalp analysis system in which a web camera, a microscope image sensor, and the Norwood–Hamilton scaling model were combined to obtain the features and parameters of images to assess the status of consumers' scalp hair. This work was implemented on the Nvidia Jetson TK1 development platform, and it is capable of simple scalp hair self-diagnosis.

Wang *et al.* [23] evaluated several machine learning and deep learning techniques for AI edge computing-based intelligent scalp hair detection. In this study, the deep learning-based ImageNet-VGG-f-model [24] and several other machine learning-based classifiers were implemented and compared. The study results showed that the accuracy achieved by deep learning-based methods is considerably higher than that achieved by machine learning-based methods. The adopted deep learning-based ImageNet-VGG-f-model achieved an accuracy of 89.77%.

Su *et al.* [2] proposed a deep learning-based intelligent scalp hair inspection and diagnosis system that adopted a VGG-net model to inspect and diagnose scalp hair problems.

The proposed system was able to evaluate five scalp hair problems, including dandruff, hair loss, bacteria, grease, and allergies. System recognition accuracy reached 90.9%.

Huang *et al.* [25] proposed a cloud-based intelligent skin and scalp hair analysis system that used various image processing techniques to detect and analyze the conditions and symptoms of the skin and scalp hair. This analysis system is capable of scalp hair sensitivity analysis, scalp hair oil analysis, scalp hair pore analysis, hair volume analysis, skin tone analysis, *etc*.

Chang *et al.* [26] designed and implemented a smartphone-based intelligent scalp hair diagnosis system that adopted deep learning techniques for the core image recognition tasks. This work used a portable 200× magnification imaging microscope with an adjustable focus connected to a smartphone. In addition, this system allowed novice users to inspect and diagnose their scalp hair health status to promote scalp hair healthcare at home.

III. THE PROPOSED SCALPEYE SYSTEM

A. SYSTEM CONSTRUCTION

Fig. 1 shows the architecture of the proposed ScalpEye system, which is composed of a portable scalp hair imaging microscope, a mobile device application, a cloud-based AI training server, and a cloud-based management platform.

FIGURE 1. Architecture of the proposed ScalpEye system.

To evaluate ScalpEye, more than 2,000 scalp hair microscopic images that included four common scalp hair symptoms were obtained from cooperating hairdressing companies in Taiwan. The professional physiotherapists from these cooperating hairdressing companies assisted in labeling the training images of these four common scalp hair symptoms for use in the cloud-based AI deep learning training server. The specifications of the cloud-based AI deep learning training server adopted in this work are shown in Table 1.

The portable scalp hair imaging microscope supports 20-50× and 200× magnification with an adjustable focus and supports two connection interfaces: USB 2.0 and Wi-Fi wireless communication. The image sensor on the imaging microscope is a VGA sensor (640 × 480 pixels). In this study, the imaging microscope is used to capture scalp hair images at 200× magnification.

TABLE 1. Specifications of the cloud-based AI deep learning training server.

CPU	Intel Xeon Gold 6130 CPU @ 2.10 GHz x 2
GPU	Nvidia Tesla V100 32GB x 4 Computation Performance: 14.1 TFLOPS
RAM	32 GB DDR4 RAM x 16
SSD	1.92 TB x 5
OS	Ubuntu Linux v18.4
AI Framework	Google TensorFlow v1.14.0

When a scalp hair image of a user is captured at 200× magnification, the captured scalp hair image is simultaneously transmitted to the mobile device application and to the proposed cloud-based AI training server though a Wi-Fi wireless network.

The captured scalp hair image is evaluated for four common scalp hair symptoms (folliculitis, hair loss, dandruff, and oily hair) by the cloud-based AI training server. The symptom severity scores determined are transmitted to the mobile device app via Wi-Fi.

The proposed cloud-based management platform can also be used for member (user) management and to record and track symptom scores. The diagnostic results related to the symptoms can be uploaded to the proposed cloud-based management platform from the mobile device app via Wi-Fi.

B. SEVERITY SCORES FOR THE FOUR COMMON SCALP HAIR SYMPTOMS

The four common scalp hair symptoms are scored according to the severity of the symptoms. Table 2 shows the severity scoring for the four tested symptoms. The severity is divided into four levels: minor, normal, middle, and high. The severity is determined based on the symptoms; the symptom percentage is the ratio of the symptom area to the area of the captured image.

TABLE 2. Severity scoring for the four common scalp hair symptoms.

Severity Classification	Classifications of Scalp Hair Symptoms			
	Dandruff (%)	Folliculitis (%)	Hair Loss (%)	Oily Hair (%)
Minor	0~10	0~10	0~5	0~10
Normal	10~20	10~20	5~10	10~20
Middle	20-40	20-40	10-20	20~40
High	40~	40~	20~	40~

The scores are defined to reflect different severities of scalp hair symptoms. Examples of the captured 200× magnification scalp images for the four common symptoms are shown in Figs. 2–5.

Next, we describe how the severity of scalp hair symptoms are scored in this work. First, we assume a labeled symptom A_1 whose coordinates are $[x_{1\,min}, y_{1\,min}, x_{1\,max}, y_{1\,max}]$. Next, we calculate the size of the symptom area. This area passes

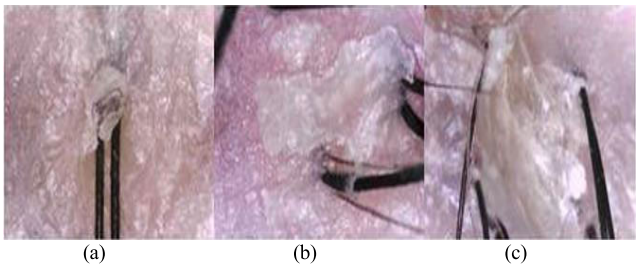

(a) (b) (c)

FIGURE 2. Dandruff symptoms: (a) Normal; (b) Middle; (c) High.

(a) (b) (c)

FIGURE 3. Folliculitis symptoms: (a) Normal; (b) Middle; (c) High.

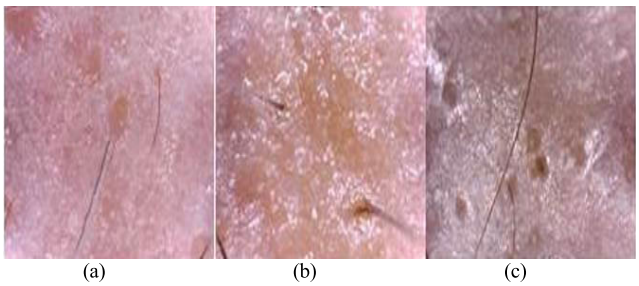

(a) (b) (c)

FIGURE 4. Hair loss symptoms: (a) Normal; (b) Middle; (c) High.

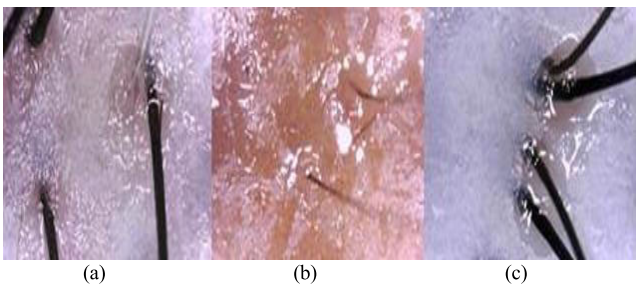

(a) (b) (c)

FIGURE 5. Oily hair symptoms: (a) Normal; (b) Middle; (c) High.

through the image area, and the classification interval determines the severity.

When symptoms overlap (as shown in Fig. 6), the second labeled symptom is set to A_2, and its coordinates are [$x_{2\,min}$, $y_{2\,min}$, $x_{2\,max}$, $y_{2\,max}$]. Then, we calculate the overlapping parts. Finally, we sum the areas for each symptom and subtract the overlapping parts. The equations corresponding to

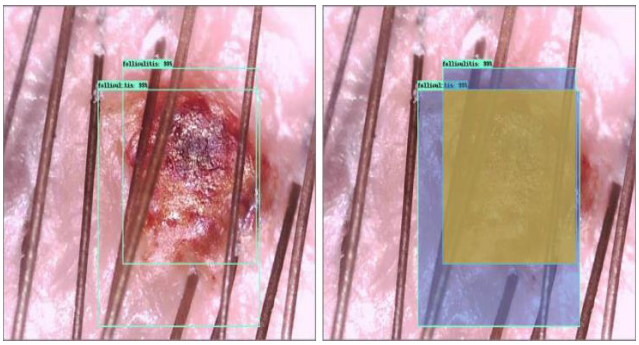

FIGURE 6. Overlapping symptoms.

this method are as follows:

$$\begin{aligned} width &= \min(x1_{max}, x2_{max}) - max(x1_{min}, x2_{min}), \\ height &= \min\left(y1_{max}, y2_{max}\right) - max(y1_{min}, y2_{min}), \\ A_{1area} &= (x1_{max} - x1_{min}) * \left(y1_{max} - y1_{min}\right), \\ A_{2area} &= (x2_{max} - x2_{min}) * \left(y2_{max} - y2_{min}\right), \\ Over_{area} &= height * length, \\ True_{area} &= A_{area} + B_{area} - Over_{area}. \end{aligned}$$

Note that $A_{2\text{area}}$ is the symptom area of area A_2. $Over_{\text{area}} = height^{*}length$ is the area of overlap. Finally, the areas of identical symptoms are subtracted, and then the overlap area is subtracted to obtain the true range of symptoms, defined as $True_{\text{area}}$.

This method for computing symptom overlap is highly suitable for determining the severity scores of scalp hair symptoms in cases where two or more identical symptoms overlap.

C. DEEP LEARNING MODEL SELECTION

To select a suitable deep learning model, we first refer to a previous comparison study [27] regarding object detection models on the COCO dataset that reported the speed and accuracy for possible candidate deep learning models. We also referred to our past works and related experience [28]–[30] to select several candidate deep learning models [31]–[35] suitable for use in this study, as follows.

(1) Faster R-CNN Inception_v2
(2) SSD Inception_v2
(3) Faster R-CNN Inception_ResNet_v2_Atrous

The architecture and features of these candidate deep learning models are briefly introduced below.

1) FASTER R-CNN INCEPTION_V2

The Faster R-CNN Inception_v2 model is based on the Faster R-CNN model [31] and uses the Inception v2 network architecture. The first stage extracts features using candidate regions. Certain intermediate features are selected to predict regions that are not related to the target category. The second stage uses these candidate regions to extract intermediate features, and finally, it feeds the clipped features back to the

feature extractor to predict the category of each candidate region and optimize specific candidate regions.

In other words, in this architecture, the Faster RCNN feature involves the introduction of the region proposal network (RPN). In the last layer of the initial CNN, a 3 × 3 sliding window moves over the entire feature map and maps it to a lower dimension (256D for visualizing and understanding convolutional networks (ZF model) [36] and 512D for the VGG-16 model [37]). In Fig. 7(a), multiple possible regions are generated by k fixed anchor boxes at each sliding window position, as shown in Fig. 7(b). Each candidate region is composed of the objectivity score of the region and the four coordinates representing the candidate frame of the region.

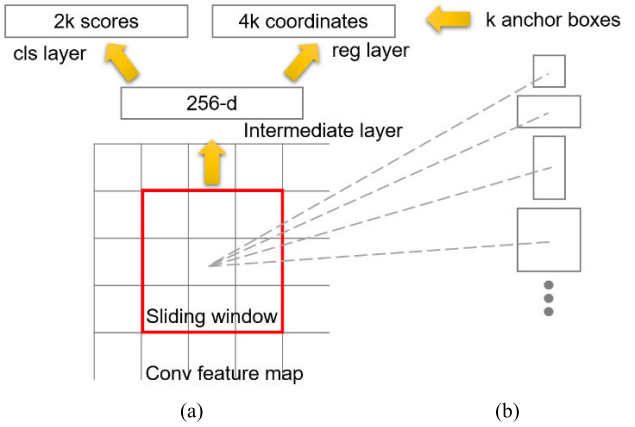

FIGURE 7. (a) Region proposal network (RPN); (b) Anchor boxes.

Fig. 8 shows the architecture of the Faster R-CNN model. Note that the Inception_v2 module in the Faster R-CNN's Inception v2 architecture is the same as the Inception v2 module in the abovementioned SSD model. The orange partition (proposal generator) in the figure indicates the RPN concept. We can use these generated anchor boxes to detect objects and refine them to a more accurate range. As shown in the green partition (box classifier) of the figure, we can give these objects an objectness score. The refined boxes are representative of the region classification.

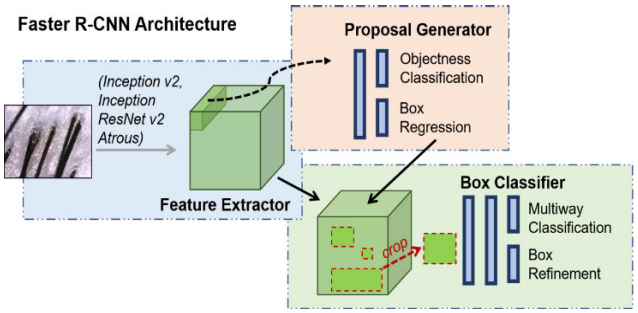

FIGURE 8. Architecture of the Faster R-CNN model.

The output of the Inception_v2 network is input into a batch normalization (BN) layer [32], which normalizes each input value. Hence, the output range is a normal distribution of N (0,1). This output is then sent to the next layer of the neural network, which solves the problem of internal covariate shift. Hence, the architecture efficiently reduces or eliminates dropout to simplify the network structure and improve the upper limit of accuracy when the model converges.

2) SSD INCEPTION_V2 MODEL

The SSD Inception_v2 model is a single-shot multi-box object detector (SSD) [33] that adopts the Inception v2 network architecture. SSD uses a feed-forward convolutional network to directly predict classes and anchor offsets without using candidate regions to extract features.

In other words, the SSD is based on a feed-forward convolutional network and uses a box with a fixed size and position. This box is similar to the anchor box of Faster R-CNN. Multiple fixed anchor boxes are set in advance, as shown in Fig. 9, and the objects in these boxes are processed, scored, and then undergo non-maximum suppression to produce the final object detection result.

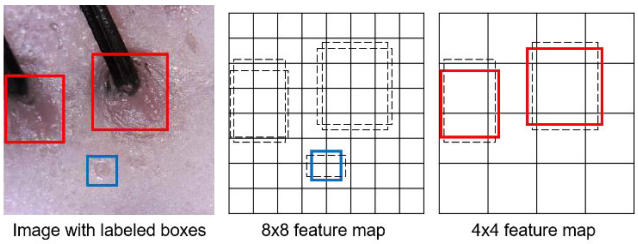

FIGURE 9. SSD uses multiple boxes with preset sizes to detect objects.

Fig. 10 shows the architecture of the SSD Inception_2 model. Unlike Faster R-CNN, the candidate region is not screened; instead, the detection result is generated directly through the feature extractor. Moreover, the Inception_v2 network architecture in SSD is the same as the Inception_v2 architecture used in the Faster R-CNN model described above.

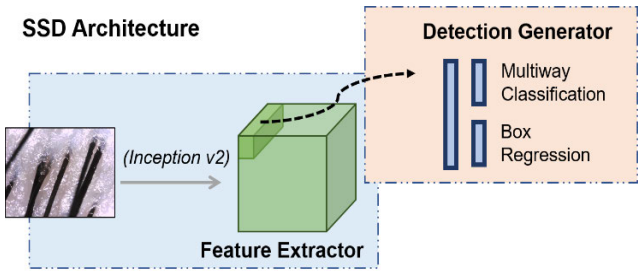

FIGURE 10. Architecture of the SSD Inception_v2 model.

In summary, SSD does not require a region proposal process; instead, it uses a fixed-size box to detect objects directly. Thus, SSD is faster than Faster R-CNN, but Faster R-CNN achieves better accuracy.

3) FASTER R-CNN INCEPTION_RESNET_V2_ATROUS MODEL

We also adopt the Faster RCNN architecture but change the Inception_v2 module to an Inception_ResNet_v2_Atrous module [35]. Inception_ResNet [33] adds the concept of a residual network based on the Inception network. Fig. 11 shows the difference between plain layers and residual block: Fig. 11(a) shows plain layers, while Fig. 11(b) shows a residual block. When $F(x) = 0$, the input X is similar to the output $H(x)$, that is, $H(x) = x$, which helps prevent the vanishing gradient problem and achieves the learning of identity mapping, ensuring that the comparisons in the subsequent layers will not result in an accuracy decline.

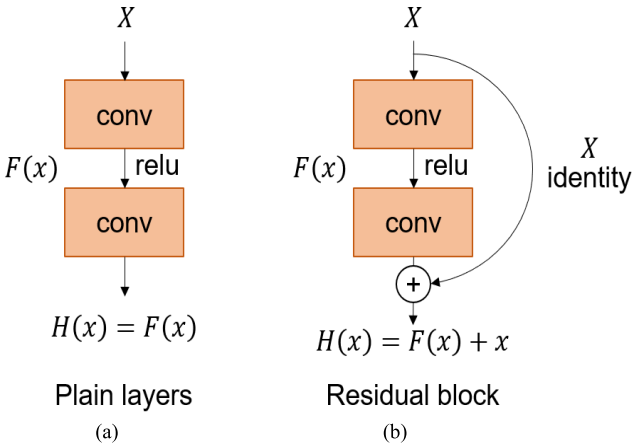

FIGURE 11. Difference between plain layers and residual block: (a) Plain layers; (b) Residual block.

A parameter called the dilated rate is introduced into the convolutional layer. This parameter defines the distance between the data processed by the convolution kernel, as shown in Fig. 12, where Fig. 12(a) is the result of ordinary pooling and Fig. 12(b) is the result of dense pooling.

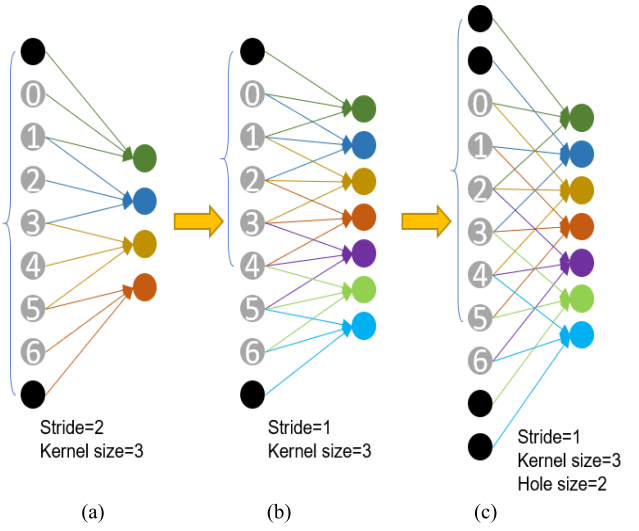

FIGURE 12. Relationship between pooling and Atrous convolution.

In Fig. 12(a), the normal convolution is assumed to have a kernel size of 3, thus the size of the receptive field will be 7, while in the same action in Fig. 12(b), the corresponding receptive field will become 5 if we use a setting of hole=2.

Atrous convolution is shown in Fig. 12(c), where the receptive field is still 7. Hence, Atrous convolution can ensure that the receptive field remains unchanged after pooling, and it can be fine-tuned while also ensuring that the output results are more refined.

The architecture of the Atrous convolutional layers is shown in Fig. 13. In the Inception_ResNet_v2_Atrous module, convolution layers based on the Atrous method are added to the Inception_ResNet_v2 architecture. As a result, the layers within the Inception_ResNet_v2 architecture use Atrous convolutions at different rates, turning the basic convolutional network into an Atrous version.

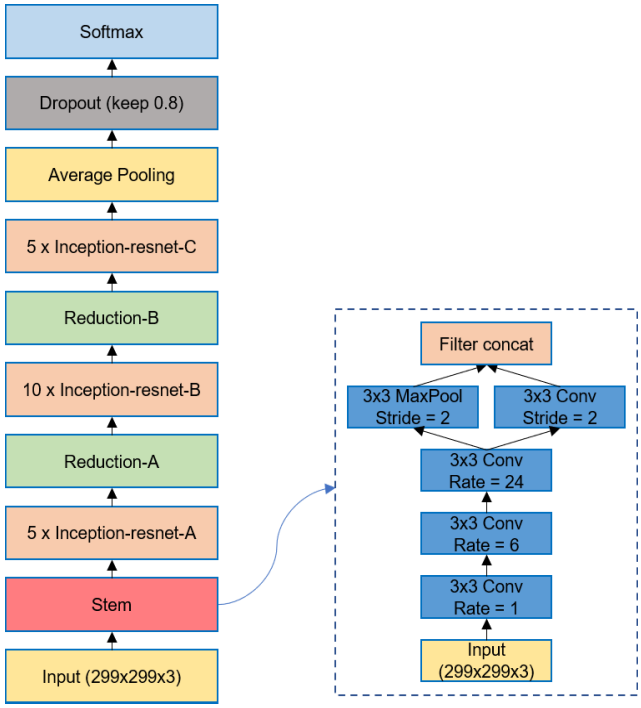

FIGURE 13. Architecture of Inception_ResNet_v2_Atrous.

D. EXPERIMENTAL ENVIRONMENT SETUP

In this experiment, we used microscopy images of scalp hair symptoms provided by experts in scalp hair care from a cooperating hairdressing company in Taiwan. The scalp hair images are 200× magnified microscope images captured by the portable scalp hair image microscope, as shown in Fig. 14.

These images are used as the deep learning training dataset for four common scalp hair symptoms. The dataset includes 615 images of dandruff symptoms, 312 images of folliculitis symptoms, 859 images of hair loss symptoms, and 412 images of oily hair symptoms. Over 2,000 microscope images of scalp hair symptoms were used in total. The experimental settings for training the AI deep learning models are listed in Table 1.

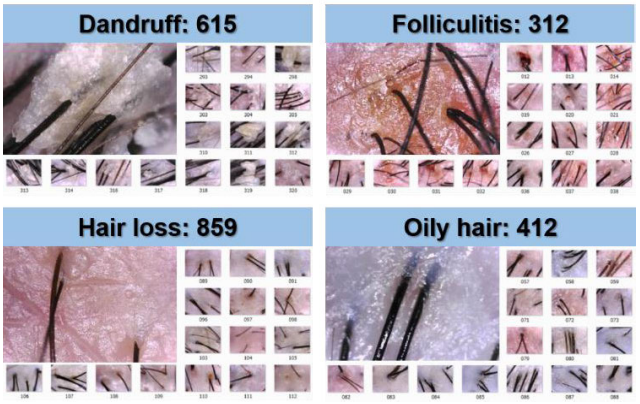

FIGURE 14. Training dataset for four common scalp hair symptoms.

Next, we used the labeling tool LabelImg to label the microscope images of the four common scalp hair symptoms. The format for the labeled microscopic images includes a scalp hair microscope image file and an XML file. The XML file content contains the tagged records for the scalp hair image file, a defined name for the frame-selected object, its coordinates, *etc*.

All the symptoms were labeled with assistance from scalp hair physiotherapists from our cooperating hairdressing company. The feature related to the four common symptoms are introduced as follows.

Dandruff is a state in which the white keratin on the scalp has not fallen off. Folliculitis involves follicular pores, inflammatory symptoms, and pustules on the hair cells. Hair loss consists of hair follicle pores without hairs or where hair growth is blocked by secretions. Oily hair shows excessive oil secretion, which leads to clogged pores. The oil reflects light.

An example of the screens used for labeling the microscopic images of scalp hair symptoms is shown in Fig. 15. The case numbers for each symptom labeled in the original scalp hair microscopic images are listed in Table 3, and include 1,235 cases of dandruff, 312 cases of folliculitis, 589 cases of hair loss, and 412 cases of oily hair.

Two approaches are adopted to ensure consistent results. (1) The imaging sample ratio is 9:1 (training to test). (2) Scalp hair physiotherapists were employed to assist in randomly checking whether the predicted outcome is correct.

IV. EXPERIMENTAL RESULTS

A. EXPERIMENTS

Table 4 describes the deep learning training process, during which each microscope image is randomly flipped horizontally to enhance the training dataset, known as data augmentation preprocessing [23].

As shown in Table 4, the number of training steps was set to 200,000. The final memory usage, training time, and processing time required by each of the three tested deep learning training models are shown in Table 4. The memory usage ranges from 87% to 90%. The training times are 8 h 46 m 18 s for SSD Inception_v2, 17 h 56 m 45 s for Faster R-CNN Inception_v2, and 32 h 36 m 34 s for Faster R-CNN Inception_ResNet_v2_Atrous, respectively.

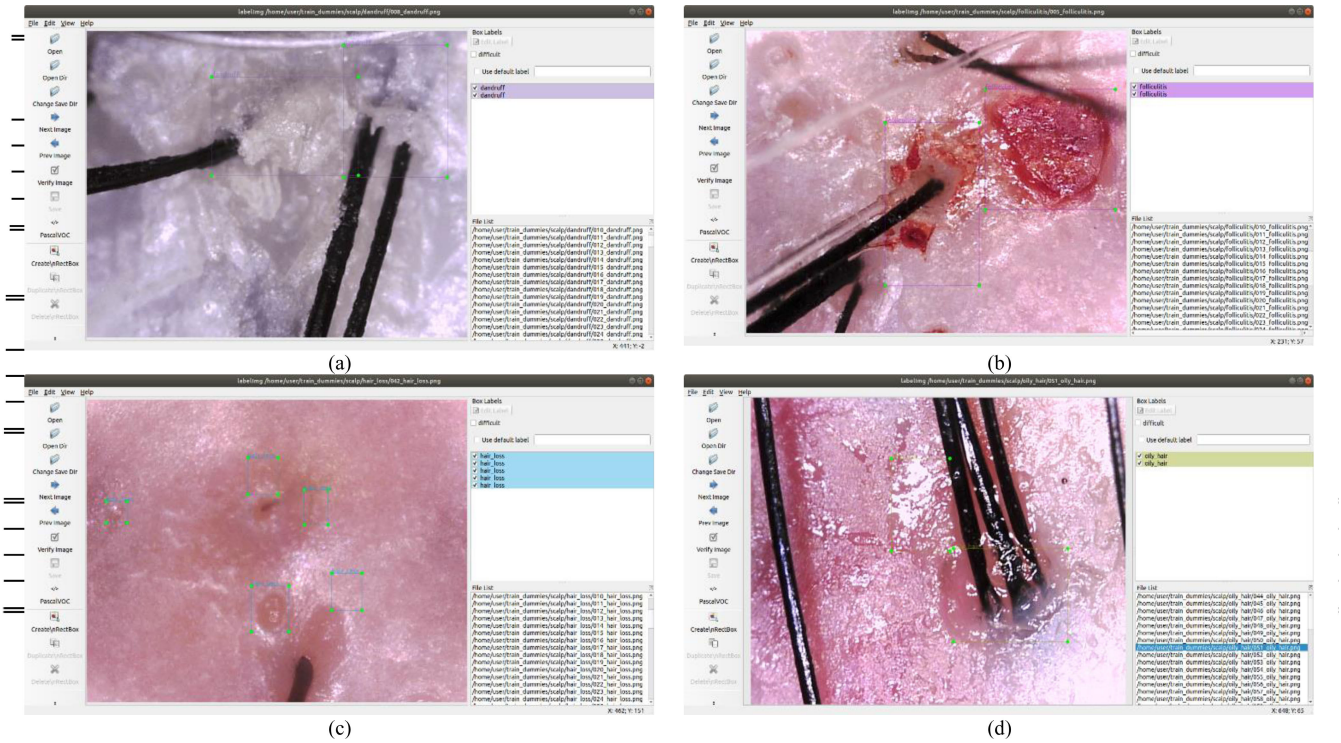

FIGURE 15. An example of the process of labeling the symptoms in the microscopic images. (a) Dandruff. (b) Folliculitis. (c) Hair loss. (d) Oily hair.

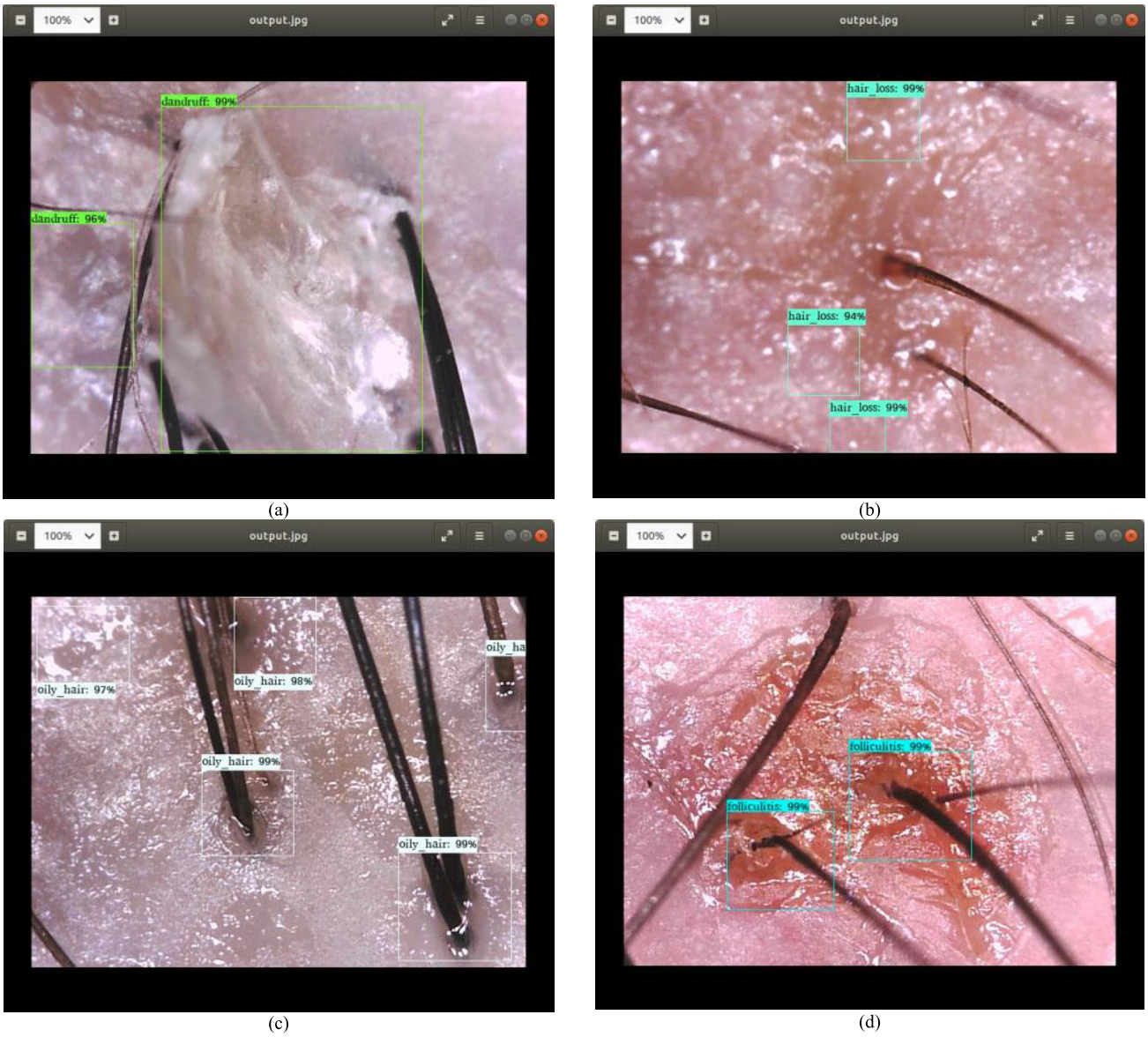

FIGURE 16. Recognition results of hairy scalp symptoms. (a) Dandruff. (b) Folliculitis. (c) Hair loss. (d) Oily hair.

TABLE 3. Hair scalp symptom recognition results.

Symptoms	Original Images	Total Cases of Symptoms Labeled from Original Images	Total Cases of Symptoms Diagnosed from Original Images		
			SSD Inception_v2	Faster R-CNN Inception_v2	Faster R-CNN Inception_v2_ResNet_ Atrous
Dandruff	615	1,235	1,128	1,191	1,203
Folliculitis	312	544	480	504	531
Hair Loss	589	2,208	1,940	2,207	2,188
Oily Hair	412	1,040	899	963	1,016

The processing time for a single scalp hair microscopic image is less than 1 second; therefore, it is difficult to measure the exact processing time. Hence, the processing time listed in Table 4 is the period of time from the initiation of processing plus the average time required for continuous processing of 100 scalp hair microscope images. The processing times for 100 microscope images are 1,025 ms (SSD Inception_v2), 1,312 ms (Faster R-CNN Inception_v2), and 5,125 ms (Faster R-CNN Inception_ResNet_v2_Atrous) for the three algorithms, respectively. Among the tested deep learning training models, the SSD Inception_v2 model achieved the fastest training and processing time; both Faster R-CNN and the Inception_ResNet_v2_Atrous model were slower.

FIGURE 17. Execution screenshots of the mobile device app of the proposed ScalpEye system.

TABLE 4. Deep learning training process.

Method	Backbone	Training Steps	Memory Usage	Training Time	Processing Time (100 images processed)
SSD	Inception_v2	200,000	87%	8h 46m 18s	1,025ms
Faster R-CNN	Inception_v2	200,000	89%	17h 56m 45s	1,312ms
Faster R-CNN	Inception_ResNet_v2_Atrous	200,000	90%	32h 36m 34s	5,125ms

Table 5 shows the average precision (AP) obtained when diagnosing the four common scalp hair symptoms using the three selected deep learning training models. The AP scores for diagnosing the four common scalp hair symptoms by the SSD Inception_v2 model range between 86.44% and 91.34%, while the Faster R-CNN Inception_v2 model AP scores range from 92.60% to 99.95% and those of the Faster R-CNN Inception_ResNet_v2_Atrous model range from 97.41% to

FIGURE 18. Scalp hair inspection and diagnosis for scalp healthcare in the hairdressing company.

TABLE 5. Average precision (AP) for diagnosing the four common scalp hair symptoms by three selected deep learning training modules.

Method	Backbone	AP [Dandruff]	AP [Folliculitis]	AP [Hair Loss]	AP [Oily Hair]
SSD	Inception_v2	91.34%	88.24%	87.86%	86.44%
Faster R-CNN	Inception_v2	96.44%	92.65%	99.95%	92.60%
Faster R-CNN	Inception_ResNet_v2_Atrous	97.41%	97.61%	99.09%	97.69%

TABLE 6. Mean average precision (mAP) for diagnosing the whole scalp hair symptoms by three selected deep learning training modules.

Method	Backbone	mAP	mAP (.50 IoU)	mAP (.75 IoU)
SSD	Inception_v2	87.16%	99.58%	96.06%
Faster R-CNN	Inception_v2	81.46%	97.89%	93.26%
Faster R-CNN	Inception_ResNet_v2_Atrous	91.75%	98.89%	96.64%

99.09%. As shown in Table 5, the Faster R-CNN Inception_ResNet_v2_Atrous model yields the best recognition results; its AP scores can reach 97.41%.

Table 6 shows the mean average precision (mAP) when the three selected deep learning training models are used to diagnose all the scalp hair symptoms; both the overall mAP and the mAP when using different intersection over union (IoU) threshold settings (.50 and.75) are shown. The Faster R-CNN_Inception_ResNet_2_Atrous model achieves the best mAP.

According to the above experimental results, we ultimately selected the faster R-CNN Inception_ResNet_v2_Atrous model to perform the core scalp hair microscope image recognition tasks in the proposed ScalpEye system. The recognition results for the four scalp hair symptoms are depicted in Fig. 16.

B. SYSTEM DEMONSTRATION

The proposed ScalpEye system was successfully applied to scalp healthcare for scalp hair inspection and diagnosis by two cooperating hairdressing companies (HairING Health Chain Group, Taiwan, and Milan Fashion Hair Group, Tainan, Taiwan).

Fig. 17 shows some screenshots of the mobile device app of the proposed ScalpEye system. Fig. 17(a) shows the member (customer) login screen. Fig. 17(b) shows the customer management list. Fig. 17(c) shows the real-time scalp hair microscopic imaging capture screen; based on this view, the image is captured by the portable scalp hair imaging microscope and transmitted to the mobile device app. Fig. 17(d) shows the scalp hair diagnosis process that performs severity scoring for the four common scalp hair symptoms. Fig. 17(e) shows the selected treatment before scalp hair care procedures. Fig. 17(f) shows the appointment times after the scalp hair care procedures.

Fig. 18 demonstrates a real application case of scalp hair inspection and diagnosis. As shown, the proposed ScalpEye system has been successfully adopted for scalp hair healthcare in the hairdressing company in Taiwan. The proposed ScalpEye system saves hairdressing companies considerable time and costs compared to continuously training haircare workers. Furthermore, the scalp hair diagnosis results are standardized for consistency and do not vary between individuals.

V. CONCLUSION

In this article, a deep learning-based scalp hair inspection and diagnosis system, named ScalpEye, is proposed for use in scalp healthcare. The proposed system is composed of a portable scalp hair imaging microscope, a mobile device

app, a cloud-based AI training server, and a cloud-based management platform.

The proposed ScalpEye currently supports the inspection and diagnosis of four common scalp hair symptoms (dandruff, folliculitis, hair loss, and oily hair). We implemented and compared three deep learning models. The experimental results showed that the Faster R-CNN Inception_ResNet_v2_Atrous model yields better recognition results in a reasonable processing time.

Based on the experimental evaluation, the Faster R-CNN Inception_ResNet_v2_Atrous model was selected as the deep learning training model and applied to inspect and diagnose the four common scalp hair symptoms in the proposed ScalpEye system. The average precision (AP) when diagnosing the four common scalp hair symptoms with the proposed ScalpEye system ranges from 97.41% to 99.09%. The proposed ScalpEye system was evaluated by two cooperating hairdressing companies (HairING Health Chain Group, Taiwan, and Milan Fashion Hair Group, Tainan, Taiwan) to assist in scalp hair inspection and diagnosis.

In future works, we plan to increase the number of samples to enhance the accuracy of the deep learning techniques. Moreover, we also plan to add more scalp hair symptoms to the ScalpEye system.

ACKNOWLEDGMENT

The authors would like to thank the HairING Health Chain Group, Taiwan, for providing the scalp photographs used as training data in this work. This article was presented in part at the IEEE GCCE, Nara, Japan, in 2018 [2], and in part at the IEEE LifeTech, Kyoto, Japan, in 2020, published in the IEEE Proceedings.

REFERENCES

[1] R. Rajput, "Understanding hair loss due to air pollution and the approach to management," *Hair: Therapy Transplantation*, vol. 5, no. 1, pp. 1–5, 2015.

[2] J.-P. Su, L.-B. Chen, C.-H. Hsu, W.-C. Wang, C.-C. Kuo, W.-J. Chang, W.-W. Hu, and D.-H. Lee, "An intelligent scalp inspection and diagnosis system for caring hairy scalp health," in *Proc. IEEE 7th Global Conf. Consum. Electron. (GCCE)*, Nara, Japan, Oct. 2018, pp. 507–508.

[3] L. Misery, N. Rahhali, M. Ambonati, D. Black, C. Saint-Martory, A.-M. Schmitt, and C. Taieb, "Evaluation of sensitive scalp severity and symptomatology by using a new score," *J. Eur. Acad. Dermatol. Venereol.*, vol. 25, no. 11, pp. 1295–1298, Nov. 2011.

[4] L. Misery, N. Rahhali, A. Duhamel, and C. Taieb, "Epidemiology of dandruff, scalp pruritus and associated symptoms," *Acta Dermato Venereol.*, vol. 93, no. 1, pp. 80–81, 2013.

[5] H. B. Allen and P. J. Honig, "Scaling scalp diseases in children," *Clin. Pediatrics*, vol. 22, no. 5, pp. 374–377, May 1983.

[6] A. Gemmeke and U. Wollina, "Folliculitis decalvans of the scalp: Response to triple therapy with isotretinoin, clindamycin, and prednisolone," *Acta Dermatovenerol Alp Pannonica Adriat*, vol. 15, no. 4, pp. 184–186, Dec. 2006.

[7] Y. Takagi, H. Takatoku, H. Terazaki, T. Nakamura, K. Ishida, and T. Kitahara, "The scalp has a lower stratum corneum function with a lower sensory input than other areas of the skin evaluated by the electrical current perception threshold," *Cosmetics*, vol. 2, no. 4, pp. 384–393, Nov. 2015.

[8] P. Kharazmi, M. I. AlJasser, H. Lui, Z. J. Wang, and T. K. Lee, "Automated detection and segmentation of vascular structures of skin lesions seen in dermoscopy, with an application to basal cell carcinoma classification," *IEEE J. Biomed. Health Informat.*, vol. 21, no. 6, pp. 1675–1684, Nov. 2017.

[9] I. Gonzalez-Diaz, "DermaKNet: Incorporating the knowledge of dermatologists to convolutional neural networks for skin lesion diagnosis," *IEEE J. Biomed. Health Informat.*, vol. 23, no. 2, pp. 547–559, Mar. 2019.

[10] Y. Gu, Z. Ge, C. P. Bonnington, and J. Zhou, "Progressive transfer learning and adversarial domain adaptation for cross-domain skin disease classification," *IEEE J. Biomed. Health Informat.*, vol. 24, no. 5, pp. 1379–1393, May 2020.

[11] M. Q. Khan, A. Hussain, S. U. Rehman, U. Khan, M. Maqsood, K. Mehmood, and M. A. Khan, "Classification of melanoma and nevus in digital images for diagnosis of skin cancer," *IEEE Access*, vol. 7, pp. 90132–90144, 2019.

[12] Y. Gao and R. Zoughi, "Millimeter wave reflectometry and imaging for noninvasive diagnosis of skin burn injuries," *IEEE Trans. Instrum. Meas.*, vol. 66, no. 1, pp. 77–84, Jan. 2017.

[13] F. Topfer, L. Emtestam, and J. Oberhammer, "Long-term monitoring of skin recovery by micromachined microwave near-field probe," *IEEE Microw. Wireless Compon. Lett.*, vol. 27, no. 6, pp. 605–607, Jun. 2017.

[14] F. Navarro, M. Escudero-Vinolo, and J. Bescos, "Accurate segmentation and registration of skin lesion images to evaluate lesion change," *IEEE J. Biomed. Health Informat.*, vol. 23, no. 2, pp. 501–508, Mar. 2019.

[15] W. Liu, D. Jia, J. Zhao, H. Zhang, T. Liu, Y. Zhang, and Y. Sun, "An optical fiber-based data-driven method for human skin temperature 3-D mapping," *IEEE J. Biomed. Health Informat.*, vol. 23, no. 3, pp. 1141–1150, May 2019.

[16] F. Lacarrubba, G. Micali, and A. Tosti, "Scalp dermoscopy or trichoscopy," in *Alopecias-Practical Evaluation and Management, Current Problems Dermatology*, vol. 47. Basel, Switzerland: Karger, 2015, pp. 21–32.

[17] L. Rudnicka, A. Rakowska, M. Kurzeja, and M. Olszewska, "Hair shafts in trichoscopy: Clues for diagnosis of hair and scalp diseases," *Dermatologic Clinics*, vol. 31, no. 4, pp. 695–708, Oct. 2013.

[18] H. Kim, W. Kim, J. Rew, S. Rho, J. Park, and E. Hwang, "Evaluation of hair and scalp condition based on microscopy image analysis," in *Proc. Int. Conf. Platform Technol. Service (PlatCon)*, Busan, South Korea, Feb. 2017, pp. 1–4.

[19] H.-C. Shih, "An unsupervised hair segmentation and counting system in microscopy images," *IEEE Sensors J.*, vol. 15, no. 6, pp. 3565–3572, Jun. 2015.

[20] H.-C. Shih and B.-S. Lin, "Hair segmentation and counting algorithms in microscopy image," in *Proc. IEEE Int. Conf. Consum. Electron. (ICCE)*, Las Vegas, NV, USA, Jan. 2015, pp. 612–613.

[21] H. Benhabiles, K. Hammoudi, Z. Yang, F. Windal, M. Melkemi, F. Dornaika, and I. Arganda-Carreras, "Deep learning based detection of hair loss levels from facial images," in *Proc. 9th Int. Conf. Image Process. Theory, Tools Appl. (IPTA)*, Istanbul, Turkey, Nov. 2019, pp. 1–6.

[22] S.-H. Lee and C.-S. Yang, "An intelligent hair and scalp analysis system using camera sensors and norwood-hamilton model," *Int. J. Innov. Comput. Inf. Control*, vol. 14, no. 2, pp. 503–518, 2018.

[23] W.-C. Wang, L.-B. Chen, and W.-J. Chang, "Development and experimental evaluation of machine-learning techniques for an intelligent hairy scalp detection system," *Appl. Sci.*, vol. 8, no. 6, p. 853, May 2018.

[24] K. Chatfield, K. Simonyan, A. Vedaldi, and A. Zisserman, "Return of the devil in the details: Delving deep into convolutional nets," in *Proc. Brit. Mach. Vis. Conf.*, Nottingham, U.K., 2014, pp. 1–12.

[25] W.-S. Huang, B.-K. Hong, W.-H. Cheng, S.-W. Sun, and K.-L. Hua, "A cloud-based intelligent skin and scalp analysis system," in *Proc. IEEE Vis. Commun. Image Process. (VCIP)*, Taichung, Taiwan, Dec. 2018, pp. 1–5.

[26] W.-J. Chang, M.-C. Chen, L.-B. Chen, Y.-C. Chiu, C.-H. Hsu, Y.-K. Ou, and Q. Chen, "A mobile device-based hairy scalp diagnosis system using deep learning techniques," in *Proc. IEEE 2nd Global Conf. Life Sci. Technol. (LifeTech)*, Mar. 2020, pp. 145–146.

[27] Pkulzc, V. Rathod, and N. Wu. *Tensorflow Detection Model Zoo*. Accessed: Jun. 26, 2019. [Online]. Available: https://github.com/tensorflow/models/blob/master/research/object_detection/g3doc/detection_model_zoo.md

[28] W.-J. Chang, L.-B. Chen, C.-H. Hsu, C.-P. Lin, and T.-C. Yang, "A deep learning-based intelligent medicine recognition system for chronic patients," *IEEE Access*, vol. 7, pp. 44441–44458, 2019.

[29] W.-J. Chang, L.-B. Chen, and K.-Y. Su, "DeepCrash: A deep learning-based Internet of Vehicles system for head-on and single-vehicle accident detection with emergency notification," *IEEE Access*, vol. 7, pp. 148163–148175, 2019.

[30] W.-J. Chang, L.-B. Chen, C.-H. Hsu, J.-H. Chen, T.-C. Yang, and C.-P. Lin, "MedGlasses: A wearable Smart-Glasses-Based drug pill recognition system using deep learning for visually impaired chronic patients," *IEEE Access*, vol. 8, pp. 17013–17024, 2020.

[31] S. Ren, K. He, R. Girshick, and J. Sun, "Faster R-CNN: Towards real-time object detection with region proposal networks," *IEEE Trans. Pattern Anal. Mach. Intell.*, vol. 39, no. 6, pp. 1137–1149, Jun. 2017.
[32] S. Ioffe and C. Szegedy, "Batch normalization: Accelerating deep network training by reducing internal covariate shift," in *Proc. Int. Conf. Mach. Learn.*, vol. 37. Jul. 2015, pp. 448–456.
[33] W. Liu, D. Anguelov, D. Erhan, C. Szegedy, S. Reed, C.-Y. Fu, and A. C. Berg, "SSD: Single shot multibox detector," in *Proc. Eur. Conf. Comput. Vis. (ECCV)*, Sep. 2016, pp. 21–37.
[34] C. Szegedy, S. Ioffe, V. Vanhoucke, and A. Alemi, "Inception-v4, inception-resnet and the impact of residual connections on learning," in *Proc. 31st AAAI Conf. Artif. Intell. (AAAI)*, Feb. 2017, pp. 4278–4284.
[35] L.-C. Chen, G. Papandreou, I. Kokkinos, K. Murphy, and A. L. Yuille, "DeepLab: Semantic image segmentation with deep convolutional nets, atrous convolution, and fully connected CRFs," *IEEE Trans. Pattern Anal. Mach. Intell.*, vol. 40, no. 4, pp. 834–848, Apr. 2018.
[36] D. Zeiler and R. Fergus, "Visualizing and understanding convolutional networks," in *Proc. Eur. Conf. Comput. Vis. (ECCV)*, 2014, pp. 818–833.
[37] K. Simonyan and A. Zisserman, "Very deep convolutional networks for large-scale image recognition," in *Proc. Int. Conf. Learn. Represent. (ICLR)*, 2015, pp. 1–14.
[38] K. He, X. Zhang, S. Ren, and J. Sun, "Deep residual learning for image recognition," in *Proc. IEEE Conf. Comput. Vis. Pattern Recognit. (CVPR)*, Jun. 2016, pp. 770–778.

WAN-JUNG CHANG (Member, IEEE) received the B.S. degree in electronic engineering from the Southern Taiwan University of Science and Technology, Tainan, Taiwan, in 2000, the M.S. degree in computer science and information engineering from the National Taipei University of Technology, Taipei, Taiwan, in 2003, and the Ph.D. degree in electrical engineering from National Cheng Kung University, Tainan, in 2008. He is currently an Associate Professor with the Department of Electronic Engineering, Southern Taiwan University of Science and Technology, where he is also the Director of the Artificial Intelligence Over the Internet of Things Applied Research Center (AIoT Center) and the Internet of Things Laboratory (IoT Laboratory). His research interests include cloud/IoT/AIoT systems and applications, protocols for heterogeneous networks, and WSN/high-speed network design and analysis. He received the Best Paper Award from the IEEE ChinaCom, in 2009, the Best Paper Award from ICCPE, in 2016, the First Prize of the Excellent Demo Award from the IEEE GCCE, from 2016 to 2018, the First Prize Best Paper Award from the IEEE ICASI, in 2017, and the Outstanding Paper Award from the IEEE LifeTech, in 2020.

LIANG-BI CHEN (Senior Member, IEEE) received the B.S. and M.S. degrees in electronic engineering from the National Kaohsiung University of Applied Sciences, Kaohsiung, Taiwan, in 2001 and 2003, respectively, the Ph.D. degree in computer science and engineering from National Sun Yat-sen University, Kaohsiung, in 2010, and the Ph.D. degree in electronic engineering from the Southern Taiwan University of Science and Technology, Tainan, Taiwan, in 2019. In 2008, he held an Internship with the Department of Computer Science, National University of Singapore, Singapore. He was a Visiting Researcher with the Department of Computer Science, University of California at Irvine, Irvine, CA, USA, from 2008 to 2009. He was also with the Department of Computer Science and Engineering, Waseda University, Tokyo, Japan, in 2010. In 2012, he joined BXB Electronics Company Ltd., Kaohsiung, as a Research and Development Engineer, where he was an Executive Assistant to the Vice President, from 2013 to 2016. In 2016, he joined the Southern Taiwan University of Science and Technology, as an Assistant Research Fellow and an Adjunct Assistant Professor. In 2020, he joined the Department of Computer Science and Information Engineering, National Penghu University of Science and Technology, Penghu, Taiwan, as an Assistant Professor. He is a member of IEICE and PMI. He was also a TPC Member, an IPC Member, and a Reviewer of many the IEEE/ACM international conferences and journals. He received the Honorable Mention Award from the IEEE ICAAI, in 2016, the Second Prize Excellent Poster Award from the IEEE GCCE, in 2016, the First Prize Excellent Demo Award from the IEEE GCCE, from 2016 to 2018, the First Prize Best Paper Award from the IEEE ICASI, in 2017, and the Outstanding Paper Award from the IEEE LifeTech, in 2020. He was a recipient of the 2014 IEEE Education Society Student Leadership Award, the Publons Peer Review Award, from 2018 to 2019, and the 2019 Young Scholar Potential Elite Award from the National Central Library, Taiwan. Since 2019, he has serving as an Associate Editor for IEEE Access and a Guest Editor for *Energies* and *Applied Sciences* Journals.

MING-CHE CHEN (Member, IEEE) received the B.S. and M.S. degrees in computer science from Tunghai University, Taichung, Taiwan, in 2003 and 2006, respectively, and the Ph.D. degree from the Institute of Computer and Communication Engineering (CEE), National Cheng Kung University (NCKU), Tainan, Taiwan, in 2014. He was an Engineer conducting research and development on the industrial Internet of Things (IoT) with the Information and Communications Research Laboratories (ICRL), Industrial Technology Research Institute (ITRI), Southern Taiwan Innovation and Research Park, Ministry of Economic Affairs (MOEA), Taiwan, since 2014. In May 2018, he joined the Department of Electronic Engineering, Southern Taiwan University of Science and Technology (STUST), Tainan, as an Assistant Research Fellow and an Adjunct Assistant Professor. His current research interests include artificial intelligence over the Internet of Things (AIoT), the industrial Internet of Things (IIoT), cloud-based application system design, wireless sensor networks, and wireless networks. He received the Outstanding Paper Award from the IEEE LifeTech, in 2020.

YI-CHAN CHIU received the B.S. degree in electronic engineering from the Southern Taiwan University of Science and Technology, Tainan, Taiwan, in 2017, where he is currently pursuing the M.S. degree in electronic engineering. He is also an Exchange Graduate Student with the Electrical Engineering and Electronics Program, Graduate School of Engineering, Kogakuin University of Technology and Engineering (KUTE), Tokyo, Japan. His current research interests include the IoT and deep learning applications for diagnosing scalp hair symptoms. He received the Outstanding Paper Award from the IEEE LifeTech, in 2020.

JIAN-YU LIN received the B.S. degree in electronic engineering from the Southern Taiwan University of Science and Technology, Tainan, Taiwan, in 2018, where he is currently pursuing the M.S. degree in electronic engineering. His current research interests include the IoT-based LP-WAN communications protocol design, cloud-based management platform development, web-based programming, and mobile device app development.